

Modelling dark current and hot pixels in imaging sensors

Antonio Forcina, Dipartimento di Economia,
Paolo Carbone, Dipartimento di Ingegneria,
University of Perugia, Italy

November 7, 2018

Abstract

A gaussian mixture model was fitted to experimental data recorded under darkness by a camera for capturing astronomical images in order to model the distribution of hot pixels and dark current as functions of temperature and duration of exposure. The model accounts for random noise and lack of uniformity within the sensor; both components of variance are allowed to depend on experimental conditions. The results indicate that dark current does not grow linearly with respect to duration of exposure nor exponentially with respect to temperature, as claimed in the literature. In addition, interactions between the two experimental conditions are substantial. The results also provide interesting insights on the effect of temperature and duration on noise and lack of uniformity in the sensor.

Keywords. Dark current, hot pixels, dark frames, gaussian mixtures, components of variance, latent class models.

1 Introduction

Digital sensors used both in ordinary cameras and in scientific imaging suffer from several anomalies: dark current, hot pixels and thermal noise, see for instance Hochedez et al. (2014) for an accurate description based on physical models. In short, dark current denotes a signal which is present even if no light is hitting the sensor and is known to increase with duration of exposure at a rate depending on temperature. During long exposures, a very small minority of pixels may show a very high signal even in perfect darkness; these are usually called *hot pixels* because they appear very bright in a dark image; hot pixels may be seen as being occasionally defective; see Dunlap et al. (2012) for an hypothetical model of hot pixel distribution. In addition, the amount of light recorded by a given pixel is affected by quantization errors due to analog-to-digital conversion and by other random fluctuations known as *thermal noise* because it increases with temperature and duration of exposure.

All of these limitations may be almost negligible when imaging well illuminated scenes with a large signal-to-noise ratio, but they become a serious problem in many applications, like for instance astronomical images where the amount of perceivable light from nebulae or far away galaxies may be very weak and sometimes close to that of the background sky. Additionally, they may impact on other emerging technological areas, such as biometrics, where sensor ageing results in spiky shot noise pixels (see Kauba and Andreas (2017), Fridrich (2013) and Bergmüller et al. (2014)). The ordinary way of coping with these problems in

astronomical imaging is to obtain an estimate of dark current and hot pixels by averaging a set of dark frames (images taken under the same conditions but in complete darkness) and, in addition, to average several images to reduce noise, see for instance (Berry and Burnell, 2000, Chapter 6). For an overview of the literature on more sophisticated methods for coping with dark current, hot pixels and noise, see, for instance Burger et al. (2011), Chen et al. (2015), Widenhorn et al. (2010).

This paper is an attempt to formulate a reasonably flexible statistical model that describes the effect of temperature and duration of exposure on dark current, hot pixels and thermal noise. The objective in Hanselaer et al. (2014) is similar, however their models are applied to the overall averages (over pixels and images acquired under constant conditions) as depending on duration of exposure and temperature. This approach does not enable the examination of the effect of experimental conditions on ordinary and hot pixels which may react differently to temperature and duration of exposure. Because of this, here a gaussian mixture model (Fraleay and Raftery, 2002) is used. In particular, it is assumed that pixels may be of two different types and that both the mean and the variance may depend on experimental conditions. To account for the fact that the distribution of the measurement results recorded by a single pixel during a sequence of images taken under the same conditions may differ from that of other pixels due to lack of uniformity in the sensor, a model with two components of variance was used. Gaussian mixture models have been used in the analysis of dark current by Švihlík (2009), among others; his objective, however, is to design an algorithm that removes the dark current from a given image and his approach does not seem to be related to the one proposed here.

The model was applied to a set of experimental data derived from images taken under complete darkness with a monochromatic Atik 314L+, an average quality CCD (Coupled charged device) designed for astronomical imaging. The results of the analysis indicate that, once we account for the presence of hot pixels, the effects of experimental conditions on dark current do not follow a simple parametric function. Interesting insights are also provided on how thermal noise increases with temperature and duration; the experimental conditions appear also to affect the lack of uniformity of the sensor.

The paper is organized as follows: after describing the data in Section 2 and the model in Section 3, the results of the analysis are presented in Section 4.

2 The data

The experiments were performed on a monochromatic Atik 314L+ CCD camera having an array of 1392×1040 square pixels of 6.45 micron with a 16 bit analog to digital converter. In principle, after taking an image, each pixel can record an integer between 0 and $2^{16} - 1$, however the internal processor adds an offset to prevent negative values. The offset can be estimated by averaging the values recorded in an image of the shortest possible duration at lowest possible temperature.

Because exposures between 5 and 10 minutes are usual in astronomical imaging, duration of exposures were chosen to be 3, 300 and 600 seconds. Considering that the camera can be cooled up to 27° C below ambient temperature, images were taken at -10, 0 and 10 degree centigrade. By combining duration of exposure and temperature, there are 9 different experimental conditions, in addition, a set of images taken at -10° C and the minimum

allowed duration were also taken because this should correspond to conditions where dark current should be almost negligible.

For each of the 10 different experimental conditions, always under complete darkness, a sequence of 30 images were recorded in a sequence. So, altogether, the original data are made of 10×30 data matrices of size 1392×1040 . Because the original data set was rather large for being easily handled on an ordinary computer, each data matrix was first transformed into a vector of length 1,447,680 and then a random sample containing 500,000 pixels was selected and used for the 300 data vectors available; Only the data for the pixels belonging to this sample were used in the analysis.

3 The statistical model

3.1 Formulation

Suppose that, for a given experimental condition e , determined by temperature and duration of exposure, r images have been recorded in complete darkness under constant conditions on a collection of n pixels which may belong to $K = 2$ different latent types. What is observed is the digitized signal recorded by each pixel in each image.

Assume, in addition, that observations from the same pixel taken under constant conditions may be correlated. Correlation may be caused by a random effect associated with individual pixels which could make each pixel behave differently from the others in a systematic manner. For ordinary pixels this random component may be interpreted as due to some kind of imperfect uniformity of the sensor; for hot pixels it should measure persistence of anomalies during a sequence of exposures. We also assume that the tendency of a given pixel to be defective is a feature which does not depend on the experimental conditions, in the sense that temperature and duration may affect the distribution of measurement results from ordinary and hot pixels, not the probability of a given pixel being hot. Clearly, we expect that with low temperature and short exposure, the distribution of measurements from hot pixel should not be much different from that of ordinary pixels.

Let y_{iej} , $i = 1, \dots, n$, $e = 1, \dots, 10$, $j = 1, \dots, r$, denote the value recorded by the i th pixel under experimental condition e in the j th image of a sequence and \mathbf{y}_{ie} the vector with elements y_{iej} . Let also G_k denote the assumption that observations come from the k th gaussian distribution of the mixture, then

$$\mathbf{y}_{ie} | G_k \sim N(\mu_{ek}\mathbf{1}_r, \boldsymbol{\Sigma}_{ek}), \quad k = 1, 2,$$

where $\boldsymbol{\Sigma}_{ek} = v_{ek}\mathbf{I}_r + \omega_{ek}\mathbf{1}_r\mathbf{1}'_r$, \mathbf{I}_r denotes an identity matrix of size r and $\mathbf{1}_r$ is an $r \times 1$ vector of 1's. The dependence of the mean and the variance components on experimental conditions may be formulated in a flexible way within the general assumption that μ_{ek} , v_{ek} , ω_{ek} are assumed to be suitable functions of duration and temperature. To model the dependence of the two variance components on covariates, a log link may be used to ensure that estimates of variance components are non negative, (Aitkin, 1987),

$$v_{ek} = \exp(\mathbf{z}'_e \alpha_k), \quad \omega_{ek} = \exp(\mathbf{z}'_e \gamma_k),$$

where $\mathbf{z}_e = (1 \ t_e \ d_e)'$ with t_e , d_e denoting temperature and duration in the e -th experiment.

Because the dependence of μ_{ek} on temperature and duration of exposure is perhaps one of the main objective of this study, several alternative models were fitted and the estimates compared with those of a non parametric model which does not constraint the dependence into a functional form. The notion that dark current increases linearly with the duration of exposure is generally accepted in the literature, see for instance Hochedez et al. (2014), p. 2. The analysis by Hanselaer et al. (2014) seems to support this property, however their conclusions are based on examining the behaviour of the overall averages, including hot pixels. It is also well known that the rate of growth of dark current increases with temperature. For instance Hanselaer et al. (2014) used a forth degree polynomial which, however, seems to be more an attempt at fitting than interpreting the phenomenon.

Because G_k is not observed, one does not know from which latent component the distribution of \mathbf{y}_{ie} comes from, that is which pixels are defective, this is an instance of a finite mixture model with two different components: ordinary and hot pixels. It is worth noting that the assumed model implies that the property of being a defective pixel does not depend on experimental conditions which can only emphasize deviant behaviors.

Though the y_{iej} come from an analogue-to-digital conversion and are thus integers, they can actually vary between 0 and $2^{16} - 1$, thus they may be seen as almost continuous measurement results. The assumption of normality will be submitted to some scrutiny in the actual application where it emerges that the assumption seems to hold with high accuracy for ordinary pixels but may fail for hot pixels when pixels start to saturate, that is receiving an amount of signal close to their maximum capacity.

3.2 The likelihood function

Let ℓ_{iek} denote the log-likelihood for the i th pixel conditional on G_k and e ,

$$\ell_{iek} = -\frac{1}{2} \left[\log |\boldsymbol{\Sigma}_{ek}| + (\mathbf{y}_{ie} - \mu_{ek} \mathbf{1}_r)' \boldsymbol{\Sigma}_{ek}^{-1} (\mathbf{y}_{ie} - \mu_{ek} \mathbf{1}_r) - r \log(\pi) \right].$$

It is convenient to exploit the structure of $\boldsymbol{\Sigma}_{ek}$ to rewrite this expression in a way which is easier to differentiate. First notice that, because the eigenvalues of the assumed covariance matrix have an explicit form, one can write

$$\log |\boldsymbol{\Sigma}_{ek}| = (r - 1) \log(v_{ek}) + \log(v_{ek} + r\omega_{ek}).$$

The same property provides also an explicit expression for the inverse covariance matrix

$$\boldsymbol{\Sigma}_{ek}^{-1} = \frac{1}{v_{ek}} \mathbf{I}_r - \frac{\omega_{ek}}{v_{ek} v_{ek} + r\omega_{ek}} \mathbf{1}_r \mathbf{1}_r' = a_{ek} \mathbf{I}_r - b_{ek} \mathbf{1}_r \mathbf{1}_r', \text{ say.}$$

It is also convenient to expand the quadratic form in ℓ_{iek} in terms of sufficient statistics; by letting \bar{y}_{ie} denote the sample average for the i th pixel given e and $W_{ie} = (\mathbf{y}_{ie} - \mathbf{1} \bar{y}_{ie})' (\mathbf{y}_{ie} - \mathbf{1} \bar{y}_{ie})$, the within pixel covariance matrix; let also $B_{iek} = r(\bar{y}_{ie} - \mu_{ek})^2$:

$$\begin{aligned} Q_{iek} &= (\mathbf{y}_{ie} - \mathbf{1} \mu_{ek})' (a_{ek} \mathbf{I} - b_{ek} \mathbf{1}_r \mathbf{1}_r') (\mathbf{y}_{ie} - \mathbf{1} \mu_{ek}) \\ &= a_{ek} (\mathbf{y}_{ie} - \mathbf{1} \mu_{ek})' (\mathbf{y}_{ie} - \mathbf{1} \mu_{ek}) - b_{ek} r^2 (\bar{y}_{ie} - \mu_{ek})^2 \\ &= a_{ek} W_{ie} + (a_{ek} - r b_{ek}) B_{eki}. \end{aligned}$$

For notational convenience, the formulation below refers to the general case of K latent classes; let $\boldsymbol{\theta}$ be the vector whose elements are the logits of $\boldsymbol{\pi}$ with respect to the first entry. Formally we may write

$$\boldsymbol{\pi} = \exp(\mathbf{G}\boldsymbol{\theta}) / (\mathbf{1}'_K \exp(\mathbf{G}\boldsymbol{\theta})),$$

where \mathbf{G} is an identity matrix without the first column. Under the assumption that observations for the same pixel under different experimental conditions are independent conditionally on G_k , the log likelihood may be written as

$$L(\boldsymbol{\theta}, \boldsymbol{\beta}, \boldsymbol{\alpha}, \boldsymbol{\gamma}) = \sum_i \log \left[\sum_k \pi_k \exp \left(\sum_e \ell_{iek} \right) \right].$$

Let $q_{ik} = \exp(\sum_e \ell_{iek})$, \mathbf{q}_i denote the vector with elements q_{ik} and $\boldsymbol{\pi}$ the vector of prior weights. With these notations, we may write $L(\boldsymbol{\theta}, \boldsymbol{\beta}, \boldsymbol{\alpha}, \boldsymbol{\gamma}) = \sum_i \log(\boldsymbol{\pi}' \mathbf{q}_i)$.

3.3 The EM algorithm

Let E_{ik} denote the posterior probability that pixel i belong to latent type k , then the complete log likelihood to be maximized in the M-step has the form

$$L_C(\boldsymbol{\theta}, \boldsymbol{\beta}, \boldsymbol{\alpha}, \boldsymbol{\gamma}) = \sum_i \sum_k E_{ik} \log [\pi_k \mathbf{q}_{ik}],$$

this can be factorized as

$$L_C(\boldsymbol{\theta}, \boldsymbol{\beta}, \boldsymbol{\alpha}, \boldsymbol{\gamma}) = \sum_k \log(\pi_k) \sum_i E_{ik} + \sum_k \left[\sum_i E_{ik} \sum_e \ell_{iek} \right].$$

An explicit estimate may be derived for the prior probabilities: $\hat{\pi}_k = E_{.k}/E_{.}$; for the second component maximization can be applied separately for each k with respect to the corresponding parameters. So, the expression to be maximized, $L_k = \sum_i E_{ik} \sum_e \ell_{iek}$, may be written as

$$L_k = -\frac{1}{2} \sum_i E_{ik} \sum_e [(r-1) \log(v_{ek}) + \log(v_{ek} + r\omega_{ek}) + a_{ek} W_{ie} + (a_{ek} - rb_{ek}) B_{eki}].$$

with respect to the corresponding parameters. The posterior probabilities E_{ik} that pixel i belong to latent type k , are computed in the E-step as

$$E_{ik} = \frac{\pi_k q_{ik}}{\sum_k \pi_k q_{ik}}.$$

3.4 Estimation of standard errors

Because the expected information matrix could not be computed with reasonable accuracy due to numerical problems arising when computing derivatives of the manifest likelihood, a two stage bootstrap was used. In the first stage pixels were resampled. In the second stage, for each pixel in the sample, the sufficient statistics were sampled from the assumed parametric model, more precisely, let \bar{y}_{ie}^* and W_{ie}^* denote the resampled sufficient statistics for the i th pixel, then

$$\bar{y}_{ie}^* \sim N[\bar{y}_{ie}, W_{ie}/(r(r-1))] \quad W_{ie}^* \sim W_{ie} \chi_{r-1}^2 / (r-1).$$

4 Analysis of the data

4.1 Model selection

Choosing a satisfactory model for μ_{ek} turned out to be a rather difficult task, mainly because of the peculiar behaviour of hot pixels. After an initial informal exploratory analysis, three basic models were considered in detail. Let d_h , $h = 1, \dots, 4$ and t_l , $l = 1, 2, 3$ denote, respectively, duration and temperature, then a linear-exponential model with no interactions (LEN) has the form

$$\mu_e = \mu_{hl} = \beta_1 + \exp(\beta_2)d_h + \exp(\beta_3 + \beta_4 t_l),$$

where $\exp(\beta_2)$ is used to constrain the effect of duration to be non negative and β_3 , β_4 are, respectively, the intercept and scale of the effect of temperature on the log scale. A model containing interactions between temperature and duration (LEI) was formulated by allowing the intercept parameter on the log scale to depend on duration

$$\mu_e = \mu_{hl} = \beta_1 + \exp(\beta_2)d_h + \exp(\beta_{2+h} + \beta_6 t_l).$$

Finally, the non parametric model (NPM) does not impose any functional restriction so that $\mu_{hl} = \beta_{hl}$. Because the three models are nested one inside the other, model selection could be based on the likelihood ratio test or the BIC; as shown in Table 1, both measures indicate clearly that the non parametric model is best. Additional insights on the relative merits of

Table 1: *BIC and likelihood ratio for testing LEN and LEI against NPM*

	NPM	LEI	LEN
n. of parameters	33	25	21
BIC/ 10^9	1.0222	1.0224	1.0226
LR/ 10^5	–	4.2376	5.0949

Table 2: *Mean square errors between mean values estimated under NPM and the other two models, separately for ordinary and hot pixels*

Ordinary pixels		hot pixels	
LEI - NPM	LEN - NPM	LEI - NPM	LEN - NPM
1.0924	1.1521	428.6540	344.1145

the alternative models is provided by the mean square differences between estimated mean values separately for ordinary and hot pixels as in Table 2. Within ordinary pixels the two parametric models are almost equivalent and are not much worse relative to NPM; instead, within hot pixels NPM does substantially better than both the parametric models.

4.2 Main results

The effect of experimental conditions on estimated mean values for ordinary pixels are moderate; on the other hand, effects on hot pixels are substantial as emerges by examining the

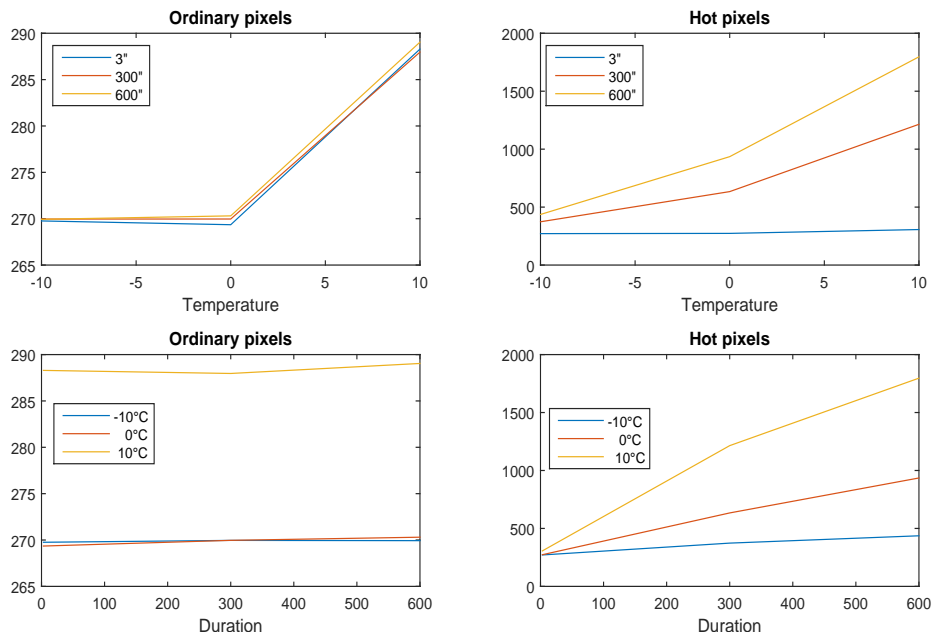


Figure 1: Plots of the mean values (estimated under NPM) versus temperature (top) and duration of exposure (bottom), separately for ordinary pixels (left) and hot pixels (right).

plot of the mean values with respect to temperature and duration in Figure 1 where the estimates from the non parametric model are displayed. The panels on the left (ordinary pixels) indicate that the effect of duration is almost negligible while that of temperature is clearly non linear. This is mainly due to the fact that exposures at 10°C suffer from a substantial amount of dark current which, instead, is hard to detect at lower temperatures. However, the effect of temperature and duration on dark current among ordinary pixels appears modest if compared to the effects recorded among hot pixels: the effects of temperature is again non linear and approximately exponential while that of duration appears also non linear but with a decreasing slope. The estimated coefficients of variation for the mean values are smaller than 0.1% among ordinary pixels and do not exceed 10% among hot pixels.

The estimates of $\sqrt{\hat{v}_k}$, $\sqrt{\hat{\omega}_k}$ are displayed in Figure 2. The value of $\sqrt{\hat{v}_k}$ may be interpreted as the sum of basic and thermal noise; it increases only slightly with temperature among ordinary pixels. Instead, among hot pixels, both temperature and duration seem to have a dramatic effect which may be interpreted as thermal noise. The estimates of $\sqrt{\hat{\omega}_k}$, due to differences between pixels, may be interpreted as a measure of the lack of uniformity in the sensor. Among ordinary pixels the effect of duration seems again negligible while that of temperature seems a little more substantial. However the situation is dramatically different among hot pixels. Here lack of uniformity is non negligible even at short exposures and low temperatures and becomes huge when both increase. This is probably due to the fact that, while certain hot pixels light up at say 1000 ADU, which is still an extremely high value, others may even reach a value close to saturation, $2^{16} - 1$. The coefficients of variation obtained from the bootstrap are well below 2% for all estimates except for certain values of $\sqrt{\hat{\omega}_k}$ among hot

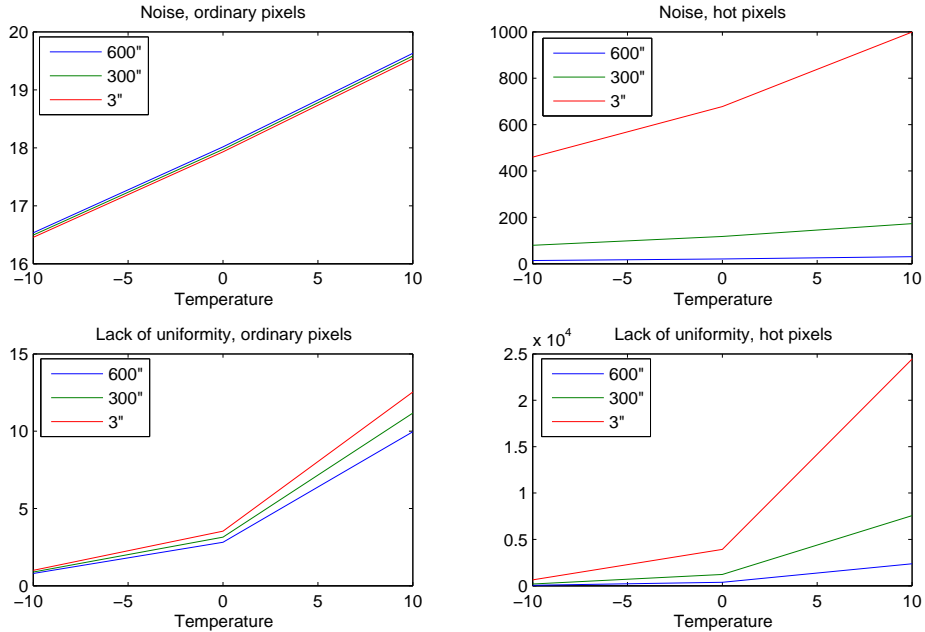


Figure 2: Plots of $\sqrt{\hat{v}_k}$ (top) and $\sqrt{\hat{\omega}_k}$ versus temperature, separately for ordinary pixels (left) and hot pixels (right).

pixels where it reaches 19%.

A set of quantile/quantile plots of residuals $\bar{y}_{ie} - \hat{\mu}_{ek}$ are displayed in Figure 3 to provide an informal critical assessment of the assumption of normality, at least for the sample averages of each set of 30 observations. It emerges clearly that averages do not depart from the assumption of normality at low temperature and duration; instead, at a medium temperature and long duration substantial divergences start to emerge even among ordinary pixels. The plot suggests that a certain proportion of ordinary pixels affected by thermal noise, diverge clearly from normality. The phenomenon becomes even more substantial with hot pixels: though there is a substantial proportion whose distribution does not seem to diverge substantially from normality, the proportion of pixels having a distribution extremely skewed to the right and occasionally close to the upper bound of $2^{16} - 1$ increases with temperature and duration of exposure.

5 Discussion

The quality of the data produced by imaging sensors, because of physical mechanisms, are affected by dark current and hot pixels which introduce bias and additional noise. The data analysed in this paper were acquired with a CCD device for astronomical imaging according to an experimental design aimed at studying the effect of temperature and duration of exposure. A finite mixture model was used to examine the behaviour of ordinary pixels, affected by dark current, separately from that of a small minority of hot pixels (estimated percentage 0.46% with a standard error of 0.01%) which appear very bright even in complete darkness. The

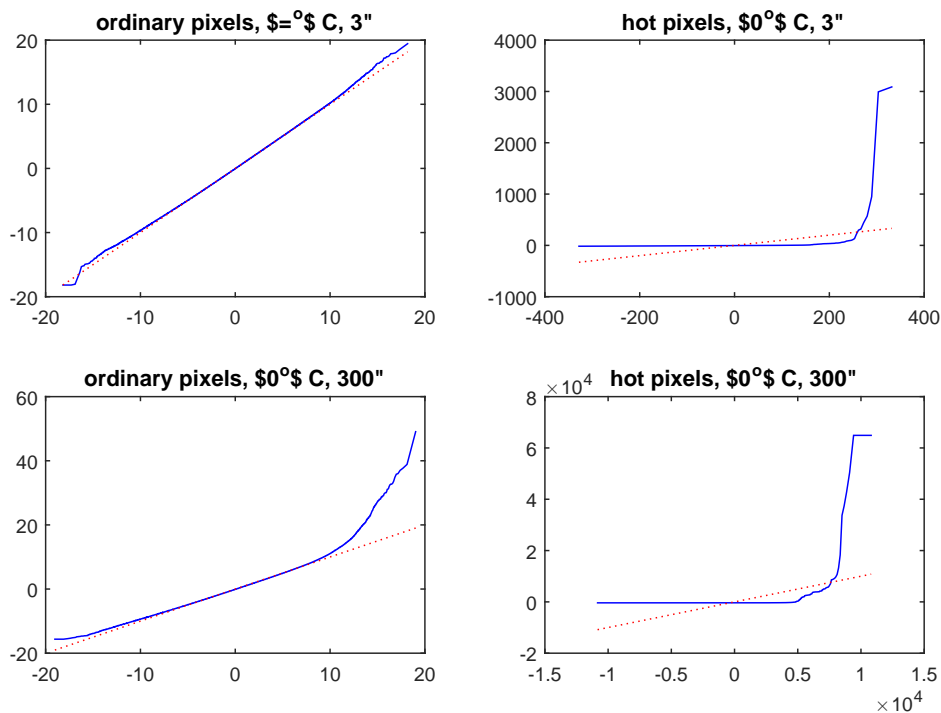


Figure 3: Quantile/quantile plot of residuals between sample averages and estimated mean values for ordinary (left) and hot (right) pixels for four specific experimental conditions.

results in 4.2 above indicate that, at reasonably low temperature, the effect of dark current among ordinary pixels is almost negligible both in terms of bias and noise.

On the whole, our results indicate that both temperature and duration of exposure have a substantial effect on the mean behaviour and noise of hot pixels. However, recent developments in the acquisition and processing of astronomical images, based on applying small random shifts of the sensor between images (so that a given hot pixels does not appear in the same position across images), combined with a suitable procedure for outlier rejection, can make hot pixels almost irrelevant.

The range of temperatures used in the experiment were limited by the fact that the Atik camera can, at most, achieve -27°C below the ambient temperature. An additional limitation in the range of experimental conditions is that, even with only 10 different experimental conditions, the whole dataset was difficult to handle; because of this, analysis was restricted to a random sample of pixels.

Some of the diagnostic plots in Figure 3 indicate that the normal distribution may not provide an adequate approximation of the distribution of the response variable under certain experimental conditions. Though this happens mainly among hot pixels which account for a small minority of the observations, it may have affected certain results. A feasible alternative might be fitting mixtures of skew normal distribution (Lee and McLachlan, 2013, see), but the implementation of these methods will require a considerable amount of additional work.

In recent years, CMOS technology is emerging as a possible improvement relative to CCD

sensors. It is well known that also CMOS sensors suffer from dark current and hot pixels, however, to the best of our knowledge, no systematic investigation comparable to the one presented in this paper has been conducted.

References

- Aitkin, M. (1987). Modelling variance heterogeneity in normal regression using glim. *Applied Statistics*, 36:332–339.
- Bergmüller, T., L., D., and et al., U. A. (2014). Impact of sensor ageing on iris recognition. In *IAPR/IEEE Int. Joint Conf. on Biometrics (IJCB'14)*. IAPR/IEEE.
- Berry, R. and Burnell, J. (2000). *Astronomical Image Processing*. Willman-Bell, Inc.
- Burger, H. C., Schölkopf, B., and Harmeling, S. (2011). Removing noise from astronomical images using a pixel-specific noise model. In *Computational Photography (ICCP), 2011 IEEE International Conference on*, pages 1–8. IEEE.
- Chen, G., Zhu, F., and Ann Heng, P. (2015). An efficient statistical method for image noise level estimation. In *Proceedings of the IEEE International Conference on Computer Vision*, pages 477–485.
- Dunlap, J. C., Blouke, M. M., Bodegom, E., and Widenhorn, R. (2012). Dark signal correction for a lukecold frame-transfer ccd-new method and application to the solar imager of the picard space mission. *IEEE Transactions on Electron Devices*, 59:1114–1122.
- Fraley, C. and Raftery, A. (2002). Model based clustering, discriminant analysis and density estimation. *Journal of the American Statistical Association*, 97:611–631.
- Fridrich, J. (2013). *Sensor defects in digital image forensic*. Springer - New York.
- Hanselaer, P., Acuna, P., Sandoval, C., Colombo, E., and Sandoval, J. (2014). Study of the dark current in a spectrograph with a ccd camera. In *ESAT - ELECTA, Electrical Energy Computer Architectures*. KU, Leuven.
- Hochedez, J.-F., Timmermans, C., Hauchecorne, A., and Meftah, M. (2014). Dark signal correction for a lukecold frame-transfer ccd-new method and application to the solar imager of the picard space mission. *Astronomy & Astrophysics*, 561:A17.
- Kauba, C. and Andreas, U. (2017). Fingerprint recognition under the influence of image sensor ageing. *IET Biometrics*, 6:245–255.
- Lee, S. X. and McLachlan, G. J. (2013). On mixtures of skew normal and skew t-distributions. *Advances in Data Analysis and Classification*, 7:241–266.
- Švihlík, J. (2009). Modeling of scientific images using gmm. *Radioengineering*, 18(4):579–586.
- Widenhorn, R., Dunlap, J. C., and Bodegom, E. (2010). Exposure time dependence of dark current in ccd imagers. *IEEE Transactions on Electron Devices*, 57(3):581–587.